Thermoreversible Gelation of Poly(Vinylidene Fluoride) in Phthalates: The Influence of Aliphatic Chain Length of Solvents

ARTICLE *in* THE JOURNAL OF PHYSICAL CHEMISTRY B · MAY 2008

Impact Factor: 3.3 · DOI: 10.1021/jp800001t · Source: PubMed

6 AUTHORS, INCLUDING:

Dr. P. Jaya Prakash Yadav
Advanced Centre of Research in High Energy …
9 PUBLICATIONS **85** CITATIONS
SEE PROFILE

Vinod K Aswal
Bhabha Atomic Research Centre
392 PUBLICATIONS **4,901** CITATIONS
SEE PROFILE

Piyush Goyal
186 PUBLICATIONS **3,678** CITATIONS
SEE PROFILE

Pralay Maiti
Indian Institute of Technology (Banaras Hind…
102 PUBLICATIONS **3,632** CITATIONS
SEE PROFILE

Thermoreversible Gelation of Poly(Vinylidene Fluoride) in Phthalates: The Influence of Aliphatic Chain Length of Solvents

P. Jaya Prakash Yadav,[†] Goutam Ghosh,[‡] Biswajit Maiti,[§] Vinod K. Aswal,[||] P. S. Goyal,[‡] and Pralay Maiti*[,†]

School of Materials Science and Technology, Institute of Technology, Department of Chemistry, Banaras Hindu University, Varanasi 221 005, India, and UGC-DAE Consortium for Scientific Research, Solid State Physics Division, Mumbai Centre, Bhabha Atomic Research Centre, Trombay, Mumbai 400 085, India

Received: January 1, 2008; In Final Form: February 4, 2008

Thermoreversible gelation of poly(vinylidene fluoride) (PVDF) has been studied in a new series of solvents (phthalates), for example, dimethyl phthalate (DMP), diethyl phthalate (DEP), dibutyl phthalate (DBP), and dihexyl phthalate (DHP) as a function of temperature and polymer concentration, both by test tube tilting and dynamic light scattering (DLS) method. The effect of aliphatic chain length (*n*) of diesters on the gelation kinetics, structure/microstructure and morphology of PVDF gels has been examined. Gelation rate was found to increase with increasing aliphatic chain length of diester. DLS results indicate that the sol−gel transformation proceeds via two-steps: first, microgel domains were formed, and then the infinite three-dimensional (3D) network is established by connecting microgels through polymer chains. The crystallites are responsible for 3D network for gelation in phthalates, and α-polymorph is formed during gelation producing higher amount of crystallinity with increasing aliphatic chain length of diester. Morphology of the networks of dried gels in different phthalates showed that fibril thickness and lateral dimensions decrease with higher homologues of phthalates. The scattering intensity is fitted with Debye−Bueche model in small-angle neutron scattering and suggested that both the correlation length and interlamellar spacing increases with *n*. A model has been proposed, based on electronic structure calculations, to explain the conformation of PVDF chain in presence of various phthalates and their complexes, which offer the cause of higher gelation rate for longer aliphatic chain length.

Introduction

Thermoreversible polymeric gels are usually formed from solution as a result of the formation of a three-dimensional (3D) network whose junction points consists of physical bonding, e.g., hydrogen-bonding or other secondary forces.[1−6] The structure of junction points (cross-link zones), morphology, and dynamical structure of these gels are usually complicated and are driven by the interaction between solvent molecules and polymer chains. Poly(vinylidene fluoride) (PVDF), possessing piezo- and pyro-electric properties, is known to have at least four crystalline structures, depending on the crystallization conditions, whose structures have been studied in detail from X-ray diffraction measurements.[7−12] Since Cho et al.[13] reported thermoreversible gelation of PVDF in γ-butyrolactone, several groups have studied physical gelation of PVDF in various solvents as the differences in interaction between polymer and solvent may greatly affect the gelation mechanism involved.[14−20] PVDF also produces thermoreversible gels in aliphatic diesters [$(CH_2)_n$− $(COOEt)_2$].[17] The fibrillar network structure is generated due to polymer−solvent complexation, and the fibrils become thinner with increasing number of carbon atoms (*n*) in diesters. Unfortunately, there is no report of PVDF gelation in aromatic diesters. Moreover, the effect of aliphatic chain length in Ph−$COO(CH_2)_n(CH_3)$ on the gelation behavior and the insight details of the fibrils were not considered in the past.

The dynamics of polymer chains in semidilute solutions as well as in gels is a relevant problem.[21−24] The dynamic light scattering (DLS) method is used to study the gelation behavior, structure and dynamics of gels.[25−31] As the gel system exhibits nonergodic (incomplete relaxation) behavior, a time-averaged DLS measurement cannot represent the appropriate dynamics of gel, and an ensemble-averaged[32−34] will be required. These ensemble-averaged spectra from gels show either a power law decay[29] or double relaxation decay with delay time (within microsecond regime). In the double relaxation spectrum, modes are due to the fast and the slow relaxations.[31] The fast mode is attributed to the cooperative diffusion of the polymer segment (mesh) between two entangled points.[28] The slow mode shows a stretched exponential decay, and the value of the exponent decreases upon gelation.[31] The non-ergodicity of the gel medium originates due to limited movements either of the mesh segments or of the cross-link zones or both. The kinetics of gelation can also be measured from the time dependent growth of crystallites of polymer in different solvents. Thereby, one can measure the gelation rate by using DLS and compare the result from conventional test tube tilting method. Takata et al.[35] measured the gelation rate of β-lactoglobulin as a function of pH, calculating the intensity-time correlation function using power law behavior in DLS.

* To whom correspondence should be addressed. E-mail: pmaiti.mst@itbhu.ac.in.

[†] School of Materials Science and Technology, Institute of Technology, Banaras Hindu University.

[‡] UGC-DAE Consortium for Scientific Research, Mumbai Centre, Bhabha Atomic Research Centre.

[§] Department of Chemistry, Banaras Hindu University.

[||] Solid State Physics Division, Bhabha Atomic Research Centre.

10.1021/jp800001t CCC: $40.75
Published on Web 03/27/2008

The structure and morphology of PVDF gels have been investigated by few groups in various solvents like aliphatic esters, ketones, etc. Most of them reported α-polymorph of PVDF in dried gels through X-ray and FTIR studies.[14−20] The reported morphology was mostly fibrillar type. To the best of our knowledge, there is no report about the dimension (both lateral and width) of fibril and their inside constituents. Small-angle neutron scattering can reveal the microstructure of gels/dried gels, especially the correlation length, which can be related to the intercrystallite distance. Kanaya et al.[36] have investigated the structure of PVA gels by using SANS and found the scattering intensity decreases with fourth power law (Porod's law) and have 170 Å as its correlation length. Time-resolved ultrasmall-angle neutron scattering[37] suggests a phase separation of PVA gels in DMSO and established a characteristic wavelength from the peak position in the scattering pattern. Nonetheless, the microstructure details of the gels can be established from SANS experiment, but to date there is no report on PVDF gels in the literature.

In this paper, we have reported the gelation of PVDF in aromatic diesters with various aliphatic chain length, namely, dimethyl phthalate (DMP), diethyl phthalate (DEP), dipropyl phthalate (DPP), dibutyl phthalate (DBP), dihexyl phthalate (DHP), and dioctyl phthalate (DOP), and how the aliphatic chain length affects the gelation behavior and its mechanism. The gelation rate of PVDF in different phthalates has been measured using both test tube tilt method as well as DLS technique. The comparative analyses between the two methods explained the microstructural progress of sol−gel transformation in our study. Differences in gelation kinetics, morphology, and structure of PVDF gels in different phthalates have been explored for the aliphatic chain length of aromatic diesters. The structure, morphology, and thermal behavior of dried gels have also been examined using X-ray diffraction (XRD), scanning electron microscopy (SEM), and differential scanning calorimeter (DSC) and have correlated with the kinetics and behavior of PVDF gels in various phthalates. Small-angle neutron scattering (SANS) has been done to explore the detail structure of fibril patterns, dimensions, and their orientation. Finally, a mechanism has been given to explain all the gelation behavior and its kinetics through scheme and molecular modeling (electronic structure calculation).

Materials and Methods

Materials. A commercial PVDF (SOLEF 6008, Ausimont, Italy) of melt flow index 24 g/10 min at 230 °C under 5 kg load was used in this work. DMP, DEP (Loba Chieme), DPP, DBP, DHP (Merck) were distilled before use. DOP was used as received from Merck. The chemical formulas of different phthalates have been presented in Scheme 1, mentioning varying aliphatic chain length (*n*). For the preparation of gel, a predetermined amount of polymer was dissolved in weighed amount of solvent (phthalate) at 200 °C to make a homogeneous solution, and then it was quickly transferred to a fixed temperature liquid bath and until the solution completely set. Gelation behavior was studied as a function of polymer concentration, temperature, and solvent.

Gelation Methods. *(a) Test Tube Tilting (TT).* For the preparation of PVDF gels in the concentration range of 2−20% (w/v), a predetermined amount of polymer was dissolved in phthalates at 200 °C and stirred to make a homogeneous solution in a test tube of 12 mm diameter, and then it was quickly transferred to a fixed temperature liquid bath and watched until the solution completely freezes upon tilting. Here, it is to be noted that the gelation time (>1.5 min) is higher than quenching time (typically <1 min). The corresponding time where no flow of the sample was observed by tilting the test tube was considered as the gelation time,[3,7,13] and the inverse of gelation time (t_{gel}^{-1}) was taken as the gelation rate at that particular concentration and temperature. The gels looked white but the transparency increases with increasing aliphatic chain length, *n*. Gelation kinetics in DMP, DEP, DBP, and DHP at 40 °C were studied as a function of polymer concentration in a wide range. In another set of measurements, the effect of temperature on the gelation kinetics was studied on 10% (w/v) PVDF in DMP, DEP, DBP, and DHP in the temperature range 25−75 °C.

SCHEME 1: Chemical Structures of Phthalates Used in This Work with Varying Aliphatic Chain Length (*n*)

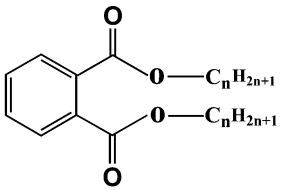

n		
1	CH_3	- Dimethyl phthalate
2	CH_2CH_3	- Diethyl phthalate
3	$(CH_2)_2CH_3$	- Dipropyl phthalate
4	$(CH_2)_3CH_3$	- Dibutyl phthalate
6	$(CH_2)_5CH_3$	- Dihexyl phthalate
8	$(CH_2)_7CH_3$	- Dioctyl phthalate

(b) Dynamic Light Scattering (DLS). DLS experiments were performed using a home-built set up, in the homodyne mode with a He−Ne vertically polarized laser ($\lambda = 632.8$ nm) source fixed at one arm of a goniometer. Samples were kept at the center of rotation of the goniometer and the photo multiplier tube detector was fixed on the other arm of the goniometer. Detail of the experimental set up can be seen in an earlier report.[35] The correlation functions from the scattered intensity fluctuation with time were generated using a 256-channel digital correlator (version 7132; Malvern, UK). Sample cell was rotated using a 12 V DC motor mounted on the sample chamber lid, and sample temperatures were controlled using a home-built temperature controller with accuracy and stability better than ± 0.5 °C. All measurements have been performed at 90° scattering angle (θ) with the sample cell rotation speed of 2 rpm. Around 30−40 spectra were collected, each for 10 s, at every concentration and temperature to get the corresponding gelation time. The detector aperture was chosen such that few speckles of the gel can be counted at a time.[34] These measurements essentially provide the dynamic structure factor (DSF) or the intermediate scattering factor (ISF), $S(q,t)$, as a function of delay time (in microsecond).

Figure 1a shows three initial DLS correlation function (i.e., $S(q,t)$ with delay time) for 10% (w/v) PVDF in DBP at 25 °C, collected at 30, 45, and 60 s, beyond which no change has been observed. The scattered intensity was also measured simultaneously at each run and plotted in Figure 1b. All $S(q,t)$ values could well be fitted with two-mode relaxation function,[38,39] for example, a fast mode with typical relaxation time $\tau_f < 100$ microseconds (μs) and a slow mode whose relaxation time ($\tau_s > 5000$ μs) diverges as gelation proceeds.[29−31] In the inset of Figure 1a, two separate modes have been shown using solid lines. The two mode relaxation function is given by the following equation:

$$S(q,t) = A_f \exp(-t/\tau_f) + A_s \exp[-(t/\tau_s)^{\beta}] \qquad (1)$$

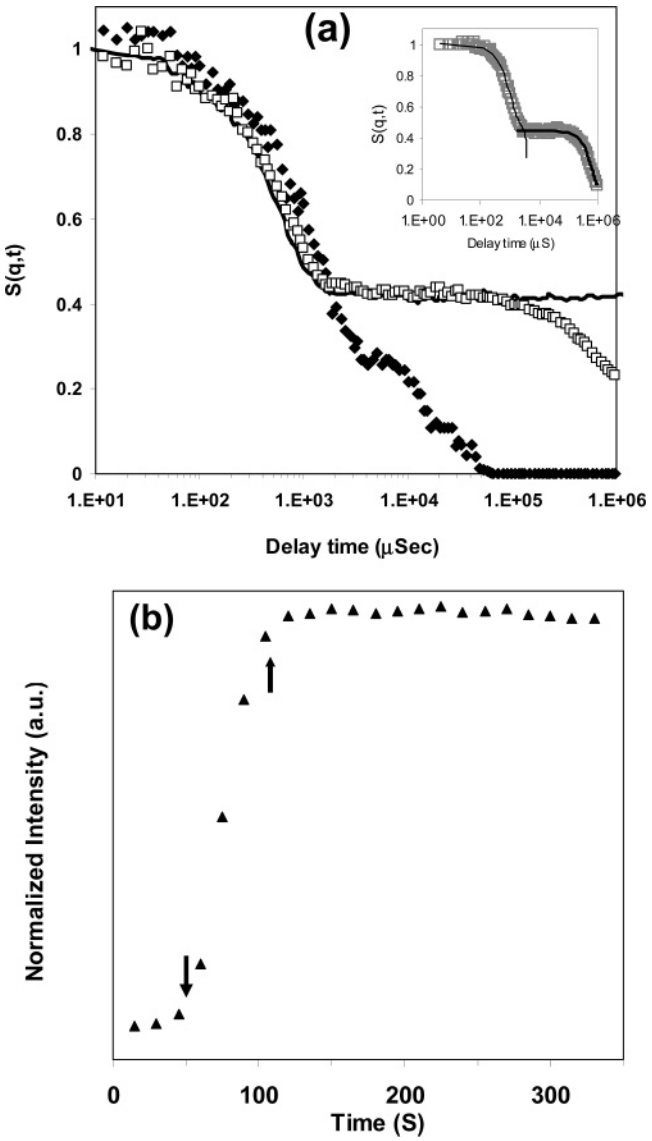

Figure 1. (a) The correlation functions, $S(q,t)$ measured at $\theta = 90°$, for 5 g dl^{-1} PVDF in DBP at 25 °C, at times (◆) 30, (□) 45, and (−) 60 s; inset shows exponential fittings of fast mode with narrow line and slow mode with thick line of the 45 s $S(q,t)$. (b) Increase in the intensity (▲) with time for the same system while transforming from sol to gel.

Subscripts f and s stand for fast and slow mode, respectively. The term A represents amplitudes where $A_f + A_s = 1$, and τ values are relaxation times, while β represents the relaxation exponent. The intensity variation with time during sol−gel transition, (Figure 1b), can be distinguished in three separate time regimes. The time regime below the downward arrow is due to diffusive mode, where the fast mode in $S(q,t)$ was significant. In the intermediate time regime, where the intensity grows up, the slow mode in $S(q,t)$ appeared significantly. As nearing to the upward arrow $S(q,t)$ function became identical. Beyond the upward arrow, that is, in the third time regime, saturation in scattered intensity was observed and the onset (at the upward arrow) was taken as the gelation point (completion of three-dimensional network), and the corresponding time was considered as the gelation time (t_{gel}). The concentration dependent gelation kinetics was measured at 40 °C. The temperature-dependent studies were performed in 10% (w/v) PVDF in every solvent

Preparation of Dried Gel. PVDF-phthalate gels were immersed in cyclohexane in a Petri dish at room temperature to replace phthalates gradually by low boiling cyclohexane. Cyclohexane was replaced by fresh set to achieve the replacement equilibrium at a faster rate in every 12 h. This process was repeated for 10 days for complete removal of phthalates from gels. After decanting cyclohexane, resulting gels were initially dried at room temperature followed by under reduced pressure at ambient temperature for 3 days to keep the morphology intact.[18] To observe the effect of guest solvent, we dried the gels only under heat treatment without using any guest solvent like cyclohexane.

X-ray Diffraction (XRD). X-ray diffraction experiments were performed using a Philips wide-angle X-ray diffractometer (DS) with Cu Kα radiation and a graphite monochromator (wavelength, $\lambda = 0.154$ nm). The generator was operated at 40 kV and 20 mA. The dried gel samples were placed on a glass sample holder at room temperature and were scanned at diffraction angle 2θ from 10 to 40° at the scanning rate of 1°/min. In a similar fashion, the diffraction studies of the gels have been carried out to know the presence of any crystallite in the gel phase after putting and leveling off the semisolid gel in the sample holder.

Differential Scanning Calorimeter (DSC). The melting temperature and heat of fusion of dried gels were measured in a Perkin-Elmer Diamond DSC instrument. The samples were heated at the scan rate of 10° min^{-1}. The peak temperature and enthalpy of fusion were measured from the endotherm using a computer attached with the instrument. The DSC was calibrated with indium before use.

Morphological Investigation. The morphology of the gels was investigated by using both scanning electron microscope (SEM) and transmission electron microscope (TEM). The surface morphology of the dried gels was examined with a LEO 435VP instrument operated at 15 kV. All the samples were gold-coated by means of a sputtering apparatus before observation. Both the thickness and lateral dimension of the fibrils were measured from several micrographs (50 distinct fibrils), and the population of fibril dimensions (both longitudinal and transverse) have been constructed in histograms. Thereafter, the distribution of fibril diameter and lateral dimension has also been constructed for various phthalates. The TEM study was done by pouring 1% (w/v) solution of PVDF in phthalates on a carbon-coated grid, followed by drying at 50 °C under vacuum for 7 days. The morphology of the gel was observed in a TEM (Philips CM-10) operated at 100KV.

Small-Angle Neutron Scattering (SANS). SANS experiments were performed on the spectrometer at the Dhruva reactor at Bhaba Atomic Research Centre, Mumbai, India.[40] The data were collected in the scattering vector (q) range of 0.017 Å^{-1} $\leq q \leq$ 0.35 Å^{-1}. The scattering from the samples were corrected for the solvent and background contributions. The whole curve as well as the lower q range was fitted separately with Debye-Bueche and other models. From the peak position in the scattering curve, the characteristics length (Λ_c) was calculated from the equation $\Lambda_c = 2\pi/q_m$, where q_m is the scattering vector q corresponding to the peak position. The temperature was kept constant at 30 °C during every measurement.

Modeling. To understand the polymer chain conformation in gels in the presence of solvents, molecular modeling has been carried out through energy minimization program to interpret intermolecular interactions involved in PVDF and phthalates with various aliphatic chain lengths. We have initially optimized α-PVDF, experimentally observed conformation, and also phthalate molecules (*cis*- and *trans*- conformations) independently. A semiempirical AM1 method, as implicated in Chem3D

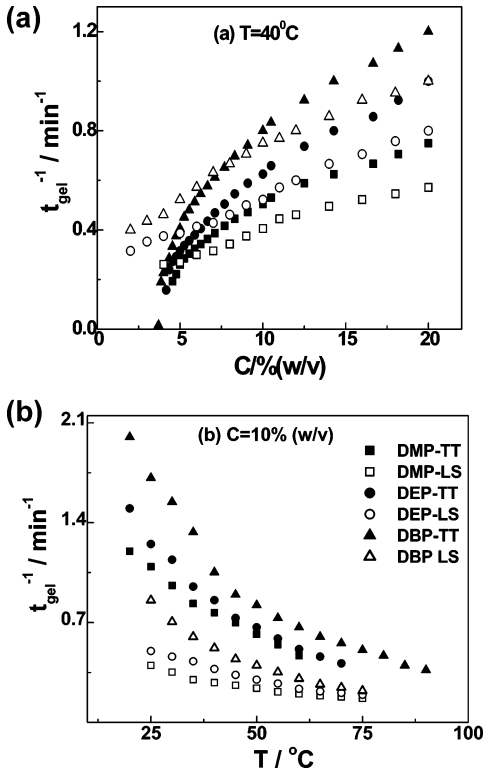

Figure 2. (a) Gelation rate versus concentration at 40 °C for PVDF in (■, □) DMP, (●, ○) DEP, and (▲, △) DBP. Closed symbols for TT method and open symbols for DLS method. (b) Gelation rate versus temperature at $C = 10$ g dl^{-1} for PVDF in (■, □) DMP, (●, ○) DEP, and (▲, △) DBP. Closed symbols for TT method and open symbols for DLS method.

Ultra 7.0, was used to obtain the optimized geometries. Those optimized structures were then used to understand the dipole−dipole interactions, believed to be the governing factor for gel formation between the >C═O groups of phthalate and $>CF_2$ groups of PVDF. We have modeled PVDF as a truncated chain consisting of minimum 12 carbon atoms.

Results and Discussion

Figure 2a shows the change in gelation rates with PVDF concentrations at 40 °C in representative three solvents, DMP, DEP, and DBP, obtained from both TT (filled symbols) and DLS (open symbols) measurements. The gelation rate decreases with decreasing concentration and the gelation rates are in the order of DMP < DEP < DBP, which indicates that the solvent with increasing aliphatic chain length ($n = 1-4$ for DMP to DBP, respectively) increases the gelation rate, raising a solvent dependency phenomena where basic nature of the solvents are same (diesters). Furthermore, the gelation rates obtained from DLS measurements showed somewhat differences in magnitude from those obtained using TT method. At high concentration regime, DLS measurements showed lower rates of gelation than TT measurements. The evolution of sol to gel is believed as combination of mainly two steps: (1) initially, several microgel clusters were uniformly formed, and (2) in the later stage, these microclusters progressively got connected together by polymer chains to form the infinite 3D network. We have carefully observed that the gelation time (time taken for the transformation from the flowing solution phase to cessation of flow or gel phase) obtained from TT method were always shorter than those obtained from DLS. So, the extra time (slower gelation kinetics) taken by the DLS may be due to the continuation of 3D networking (and corresponding increase in scattered intensity)

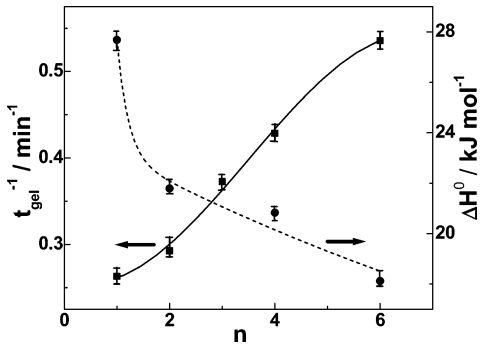

Figure 3. Gelation rate as function of aliphatic chain length (n) in diesters for polymer concentration 5% (w/v) and at 40 °C. Y_2-axis represents the heat of reactions to produce one mole of cross-link as a function of aliphatic chain length, n.

even after reaching the cessation of flow state. At low concentration regime, TT measurements showed drop in kinetics as the system reaches the cessation of flow phase at much longer time. But, amusingly, DLS measurements showed some finite values at this concentration regime. This may be due to the nucleation and growth of microgel clusters formed even at lower concentration and thereby giving similar profile in intensity versus time plots as shown in Figure 1b. Presumably because of the large separation (>1000 nm) between the microgel clusters at this low concentration regime no intercluster networking could be possible. Therefore, finite values of kinetics measured using DLS method at low PVDF concentrations should not be wrongly interpreted as infinite gelation (cessation of flow phase). We would like to mention here that the TT method is a more appropriate technique for measuring gelation rate,[3,7,13] whereas the DLS measurements usually revealed the microstructural pictures of the sol-to-gel transformation process.[41−43] Figure 2b shows the gelation rate as a function of temperature at a fixed PVDF concentration of 10% (w/v) in representative phthalates. The gelation rate increases with decreasing temperature as the formation of crystallites, necessary for gelation, are easier in case of lower temperature, as a result of higher crystallization rate at greater undercooling. Here, also the comparative rate of gelation among different solvents is same: DMP < DEP < DBP. Furthermore, the gelation rate as measured from DLS exhibits lower value because of the reason mentioned above. There are independent measurements of gelation rate of polymers by TT[15] and DLS[35] technique, but here for the first time we report their relative magnitude for PVDF-phthalate system.

Figure 3 shows the gelation rate as a function of aliphatic chain length (n) of diesters solvent used for gelation for a particular concentration of PVDF (5% (w/v)) in different phthalates by using TT method. The n value represents the number of carbon atoms in the aliphatic chain of the diesters. As mentioned earlier, the gelation rate increases with increasing the value of n. In other words, higher homologues of phthalates exhibit higher gelation rate. But, PVDF does not form gel in dioctyl phthalate (where $n = 8$) even with higher polymer concentration as observed by TT method. So, there is a limit of aliphatic chain length beyond which gelation does not occur. Further, the gelation rates in DBP (representative plot) were measured as a function of concentration at various temperatures and are shown in Figure 4. When the experimental points are extrapolated to $t_{gel}^{-1} = 0$, the value corresponding to concentration axis would provide the measure of critical gelation concentration (C_g^*). Below the C_g^*, gelation phenomena will not occur at that temperature. Contrary to the TT method, the DLS

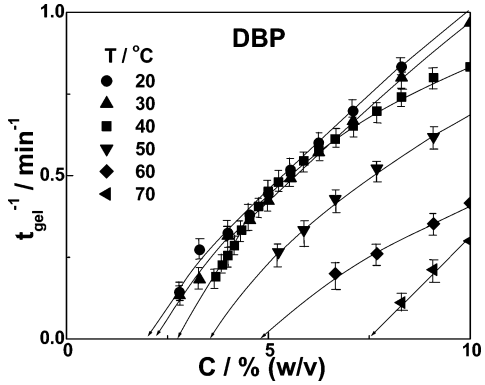

Figure 4. Representative t_{gel}^{-1} vs concentration plots in DBP solvent measured at various indicated temperatures.

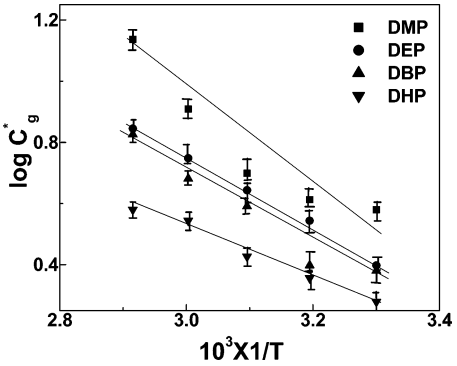

Figure 5. log C_g^* vs $1/T$ plot for indicated solvents (phthalates).

technique showed the formation of microgel clusters, as discussed above, below C_g^* though no 3D networking was taken place. The C_g^* is a function of temperature and is of interest because of the concentration, C_g^*, at which the molecular clusters begin to overlap in dilute solution. It can be easily shown that the chains are in a statistical conformation. However, the molecular overlap, which is a necessary condition for crystallization, may not be a sufficient one for gelation. The logarithmic plot (Figure 5) of log C_g^* against $1/T$ can provide the information about the heat of formation of cross-link by using the equation of Eldridge−Ferry[44]

$$\log C = \frac{\Delta H^\circ}{2.303RT} + A \tag{2}$$

where, C is the polymer concentration, ΔH° is the heat of formation of one mole of cross-link and A is a constant. We assumed that the relation holds good at the critical gelation concentration, C_g^*. The negative slope of the curves indicates the exothermic nature of the cross-link formation, which is quite obvious from the thermodynamic standpoint. The values of ΔH°*s* are 28, 22, 20.5, and 18 kJ mol^{-1} for DMP, DEP, DBP, and DHP, respectively, and are plotted in Figure 3 as a function of aliphatic chain length (n). All these values are higher than the literature reported value of 12.47 kJ mol^{-1} in γ-butyrolactone,[13] and it is proven that ΔH° is a solvent dependent parameter. Again, the gelation rate is a function of reduced overlapping concentration, ϕ, by the relation (eq 3)

$$t_{gel}^{-1} \propto \phi^n \tag{3}$$

The gelation rate versus reduced overlap concentration, defined as $\phi = (C - C_g^*/C_g^*)$, shown in the supporting document, also exhibits steeper slope with increasing aliphatic chain length of

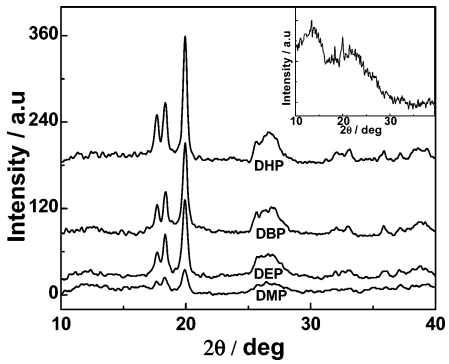

Figure 6. XRD patterns of the dried PVDF samples obtained from gels in indicated solvents. *Y*-axis has been shifted for the clarity of presentation. XRD pattern of PVDF gel in DMP solvent is shown in the inset.

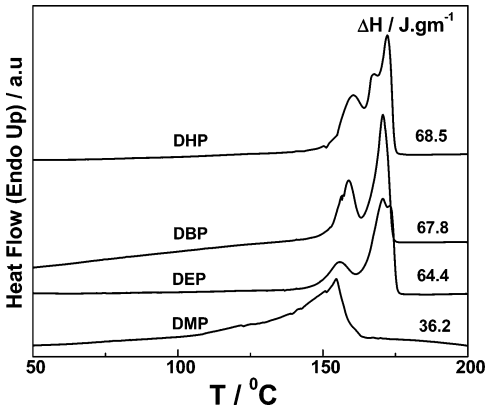

Figure 7. DSC thermographs of PVDF dried gel prepare from indicated solvents. The heating rate was at 10°/min.

diesters. The exponent of ϕ against gelation rate increases from 0.4 in DMP to 0.65 for DHP indicating that percolation in a three-dimensional lattice is a satisfactory model to explain the gelation rate of PVDF in phthalates.[15] The percolation theory predicts the exponent as 0.45 in three-dimensional lattice.[45] Our experiments were carried out not very close to critical gelation concentration to have reasonable gelation time period, which may cause this discrepancy.

Now, it is pertinent to compare the enthalpy of fusion ΔH_u° of pure PVDF with ΔH° values in a range of phthalates. The reported value of ΔH_u° is 5.95 kJ/mol for PVDF.[46] The value is much lower than the ΔH° values in all four solvents reported here. In view of the fact that crystallites act as primary points of physical junction in these gelation processes, as stated earlier it may be argued that about 5, 4, 3.5, and 3 crystallites (average value) are involved in producing a single cross-link in DMP, DEP, DBP, and DHP, respectively. So, lesser number of crystallites is needed to form the physical junction in PVDF gels in solvents with higher n value. However, it confirms the order of observed gelation rate (DHP > DBP > DEP > DMP) as the solvent with higher n value can form physical crosslinking with minimum number of PVDF crystallites, primarily needed for gelation process. It has to be remembered that the junction size is not similar to the size of the critical nucleus of the nucleation process. The former represents the size of a cross-link in the gel, and the later represents the minimum size of a nucleus, where it grows thermodynamically. Nonetheless, at least two crystallites are needed to form a cross-link junction in any gelation process. Following the decreasing order of crystallites number, required for gelation, it may be presumed that less than two crystallites are enough for polymer−solvent

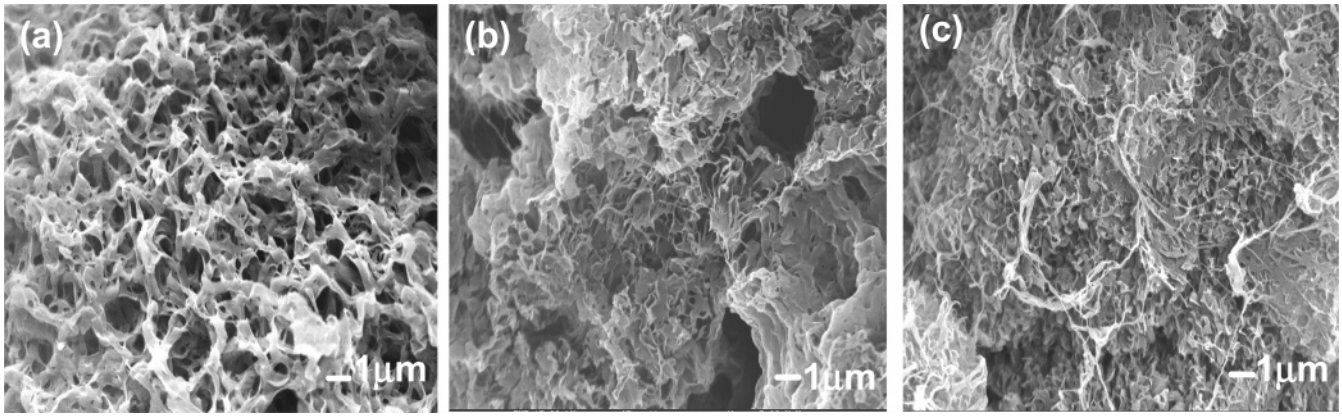

Figure 8. SEM micrographs for dried PVDF gels in (a) DMP, (b) DEP, and (c) DBP.

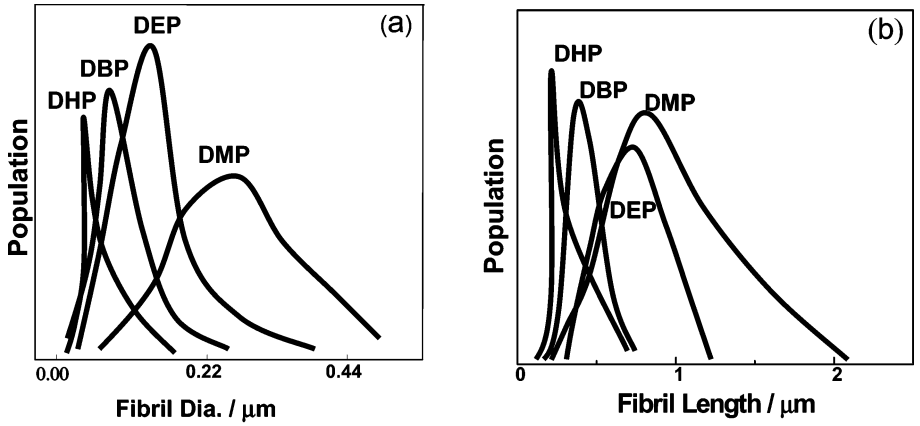

Figure 9. Distribution of fibril diameter and length obtained in different solvents (polymer concentration was 10% (w/v)).

complexes for solvents having n values higher than six, and thereby it can explain why gelation does not occur for dioctyl phthalates ($n = 8$), where the physical crosslinking of crystallites cannot take place. Dioctyl phthalate is forming strong polymer−solvent complexes but due to lack of physical crosslinking, three-dimensional network, which is necessary to generate gel, has not occurred.

Structure. The structure of the gels is determined by using XRD patterns of the dried gels. Figure 6 shows the XRD patterns of 10% (w/v) PVDF in different phthalates, and it is clear from the patterns that PVDF crystallize in α-polymorph only, irrespective of the phthalates used. Furthermore, d_{hkl} values of the dried gels are analogous with the melt-crystallized α-polymorph of PVDF.[47] The α-polymorph of the dried gels was also verified by studying the FTIR spectra of dried gels. The characteristic bands of crystalline α-phase are observed at 490, 615, 763, and 976 cm^{-1} with *TGTG* conformation.[48−50] Interestingly, crystallinity of dried gel increases in the order of increasing aliphatic chain length, as evident from the area under the respective XRD patterns. It is believed that the amount of crystallinity in gels also have the same order with different magnitude. The inset of the figure shows the diffraction pattern of gel in DMP, and it is clear that the crystallites are prominent even in presence of solvent in gels thus providing the clear evidence that gelation occurs through crystallization. Comparative weak crystalline peak in gel (inset figure) is due to less coherence of the crystallites in presence of ∼90 wt % of amorphous solvent. The crystallization phenomena, which is the precondition for gelation for these systems, is facilitated in case of higher alkane diester (higher n value), for example, DBP or DHP and the crystallizing tendency gradually decreases in the order DHP > DBP > DEP > DMP, which is the same order of gelation rate. Even though, the number of crystallites per physical junction is less in case of higher alkane diester, it exhibit higher crystallinity.

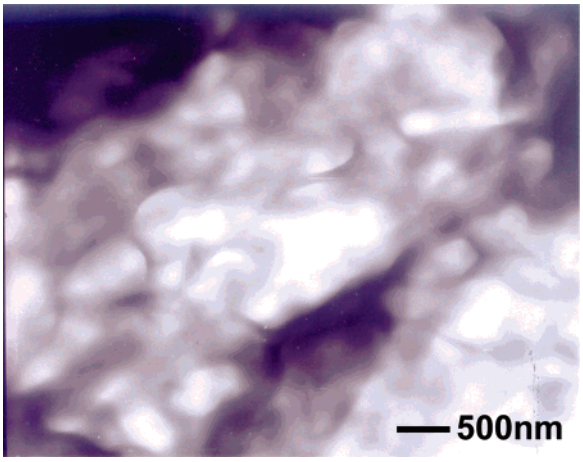

Figure 10. TEM image of PVDF gel in DBP solvent [1% (w/v)].

Thermal Behavior. Figure 7 shows the heating curves of dried gels in DSC at the heating rate of 10 °C min^{-1}. The first melting endotherm corresponds to the melting of crystallites present in dried gels. The melting temperatures are 154.4, 155.8, 158.6, and 160.0 °C for DMP, DEP, DBP, and DHP, respectively. Significant and systematic increase in melting temperature is presumably due to the perfect ordering of crystallite together with higher lamellar thickness with increasing aliphatic chain length. The double melting isotherms are explained from the melt-recrystallization phenomena of PVDF dried gels. However, the heats of fusion (ΔH) are 36, 64, 68, and 69 $J \cdot gm^{-1}$ for DMP, DEP, DBP, and DHP, respectively. Nonetheless, at par with

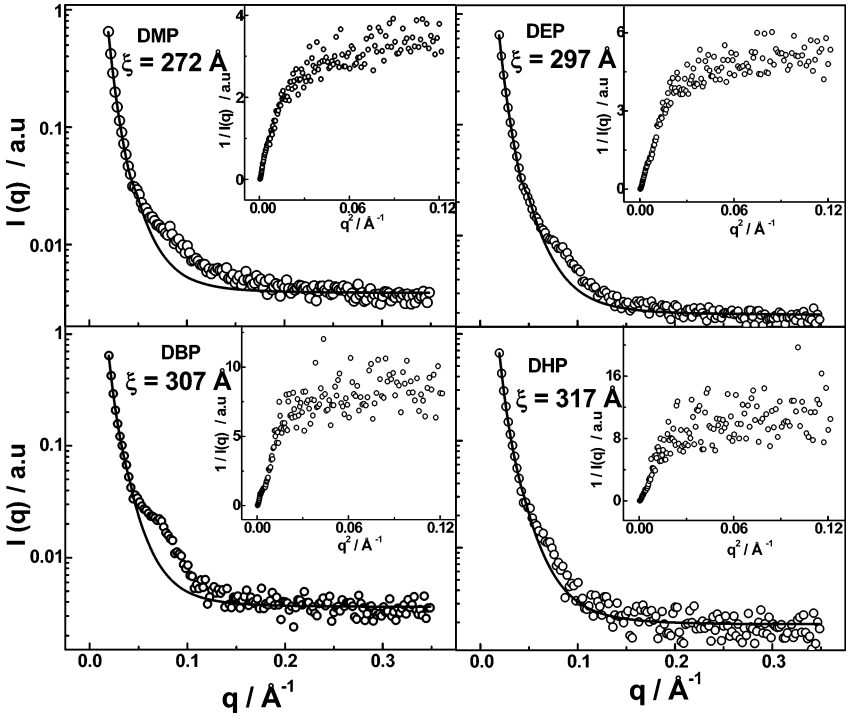

Figure 11. Small-angle neutron scattering intensity $I(q)$ of PVDF dried gels prepared from indicated solvents. The solid lines represent the Debye−Bueche fitting. The inverse of $I(q)$ is plotted against q^2 in each inset.

TABLE 1: The Correlation Length (ξ) and Characteristic Length (Λ_c) of Gels and Dried Gels in Various Phthalates Obtained from SANS Data

	ξ (Å)		Λ_c (Å)	
	dried gel	gel	dried gel	gel
DMP; $n = 1$	272	57	69	80
DEP; $n = 2$	297	61	75	83
DBP; $n = 4$	307	63	85	98
DHP; $n = 6$	317	67	89	128

the structural analysis from XRD, it is clear from thermal behavior as well that the crystallinity increases with increasing aliphatic chain length of diester.

Morphology. Surface morphologies of dried gels in three solvents have been presented in Figure 8. Clearly, the morphologies of the dried gels are of fibrillar type with decreasing fibril length and width upon increasing aliphatic chain length of diesters. Anyway, three-dimensional fibrillar network is evident for all the solvents. It is noteworthy to mention that by using low boiling guest solvent (cyclohexane), we are able to keep the original network structure present in gels, even after removing the guest solvent by very slow evaporation. Direct evaporation of phthalate from gels at higher temperature gives the collapsed structure, showing no networking in the dried gel. Direct evaporation of high boiling phthalates leads to the collapsed structure. From the histogram of the fibril diameter and its lateral dimension, the distributions have been shown in Figure 9. It is also clear that the distribution of fibril diameter gradually becomes sharp with increasing n value of various solvents. Similarly, the lateral dimension of the fibrils has also decreased with increasing n (Figure 9b). TEM image also exhibits the fibrillar pattern of the network formed in dried gel (Figure 10).

Small-Angle Neutron Scattering. The fibrillar patterns and their gradual change in dimensions are evident from the morphology. In order to look inside the fibrillar patterns, SANS has been measured to examine the detail structure. Figure 11 shows the small angle neutron scattering patterns of dried gel prepared from four indicated solvents in the q range 0.017 to 0.35 Å^{-1}. The lower and higher q regions are best fitted, represented by solid line, with Debye−Bueche model (eq 4), where $I(o)$ is the extrapolated structure factor at zero wavevector and ξ is the correlation length. Further, a distinct peak is evident in the middle portion of q for all solvents.

$$I(q) = \frac{I(o)}{(1 + \xi^2 q^2)^2} \tag{4}$$

$$I(q) = \frac{I(o)}{1 + \xi^2 q^2} \tag{5}$$

These peaks are indicative of a stacked lamellar pattern inside the fibril. Interestingly, the peak position gradually shifted to lower q range with increasing the aliphatic chain length of diesters. The characteristic lengths, $\Lambda_c = 2\pi/q_m$, are 69.1, 74.5, 84.9. and 89.1 Å for DMP, DEP, DBP, and DHP, respectively, where q_m is the wavevector corresponding to peak position. So, the gap between the lamella increases with increasing aliphatic chain length. Furthermore, the correlation lengths, ξ, have been calculated from lower q range by using Debye−Bueche model. Again, a gradual increase of correlation length is observed from 272 to 317 Å for DMP to DHP, respectively, and the values are reported in Table 1. The correlation lengths are essentially the distance between two physical crosslinking points. Now, it is obvious that more number of physical crosslinking points (lower ξ) are formed in case of lower aliphatic chain length containing diester, or in other words larger number of junction points are needed to form gel for lower aliphatic chain length diester as solvent when compared to solvents having higher n. The reciprocal of structure factor versus scattering vector has been shown in individual inset to check the validity of the other models as well. There is no ordered plateau at higher q range, which indicates that the experimental data do not fit the Ornstein−Zernike model (eq 5) while lower q range fits well with Debye−Bueche model. This set of fitting also provide the

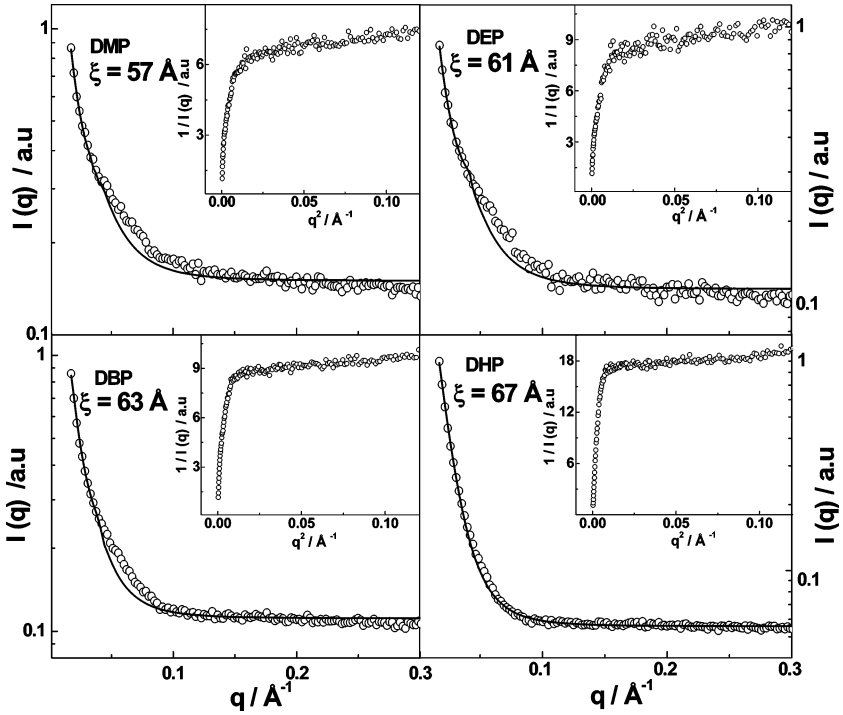

Figure 12. Small-angle neutron scattering intensity $I(q)$ of PVDF gels prepared from indicated solvents. The solid lines represent the Debye−Bueche fitting. The inverse of $I(q)$ is plotted against q^2 in insets.

SCHEME 2: Comparison of Individual Fibril (Upper Layer, Taken from SEM Micrographs) and Schematic of Lamellar Orientation Inside Fibril Showing Crystallites in Indicated Solvents

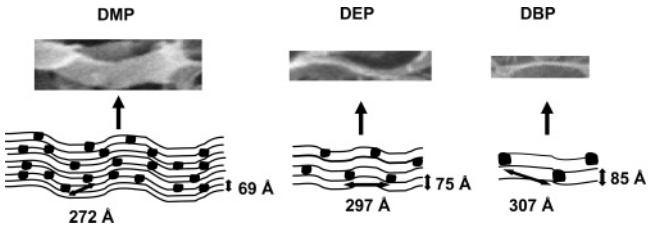

correlation length from the slope, but it contains the term, $I(o)$, extrapolated structure factor at zero wavevector.

Neutron scattering patterns for gels in presence of solvent are shown in Figure 12. The patterns are almost same with dried gel patterns. Here again, the characteristic length, Λ_c and correlation length, ξ, follow the same trend but different in magnitude and are also presented in Table 1. The difference of gels and dried gels is presumably due to the homogeneous system in gels as we used hydrogenated solvent instead of a deuterated one. In dried gel systems, the good contrast arises from inhomogeneity caused by the presence of air in place of solvent in dried gels. On the basis of the combined SANS results and SEM micrographs, the distribution of lamellae inside each fibril has been shown in Scheme 2 for various phthalates depending on aliphatic chain length. The upper parts of the model are taken from one individual fibril of SEM micrograph of respective solvent. The second layer is the schematic distribution of lamella, which combines together along with the physical crosslinking points, makes the above fibril. The black spheres are the physical junction points and solid lines are the organized lamella. As from the SANS results, simultaneously the interlamellar distance, Λ_c and correlation length, ξ, increase with increasing aliphatic chain length, *n*. SANS studies provide the insight lamellar structure of fibril and the correlation length of gels prepared from various phthalates, which also supports the thermodynamic evidence (ΔH decreases with *n* in Figure 3) that less number of crystallites are involved in gelation for phthalates having higher *n*.

Molecular Modeling. An idea about the model structure of PVDF−diester complexes may be obtained by using semiempirical AM1 (electronic structure calculations) method. First, both the structure of polymer and diester was energetically minimized. For PVDF, the particular $TGT\bar{G}$ conformation was used as the XRD pattern and FTIR spectra show only α-polymorph of PVDF in dried gels. The diester molecules can approach toward α-PVDF chain either in cis- or trans- conformation as the energy difference between the two is quite small (less than 1 kcal/mol) and conformational transformation may occur during geometry optimization. It is worth pointing out here that the trans- form of phthalate prefers double strand of α-PVDF, while the cis- form prefers only single strand of α-PVDF. It is believed that the interacting sites of PVDF and diester are the $>CF_2$ and $>C{=}O$ moieties, respectively, through which dipole−dipole type of interactions exist due to electronic polarization. Representative optimized complexes in DMP and DHP have been shown in Figure 13 using the double strand of PVDF and trans-diesters. The dashed lines show the distance between the nearest interacting sites for both strand of α-PVDF. In one side of diester, the distance becomes same (3.811 Å) for all the phthalates, while the other distance gradually decreases with increasing aliphatic chain length, *n*. The lower distance of dipoles has been plotted against aliphatic chain length in Figure 14. Interestingly, the distance gradually decreases up to $n = 6$, and then it starts increasing for double stranded model. Further, our calculation revealed that in case of cis- form of phthalates with single strand of α-PVDF, the distance between the dipoles did not change with chain length of the ester groups, indicating that interaction of *cis*-phthalate with α-PVDF plays hardly any significant role in gel formation. If we recall the experimental gelation rate, it increases up to $n = 6$ and then it does not form gel at all. The models of the complexes formed from various trans- forms of diesters and double strand α-PVDF corroborate

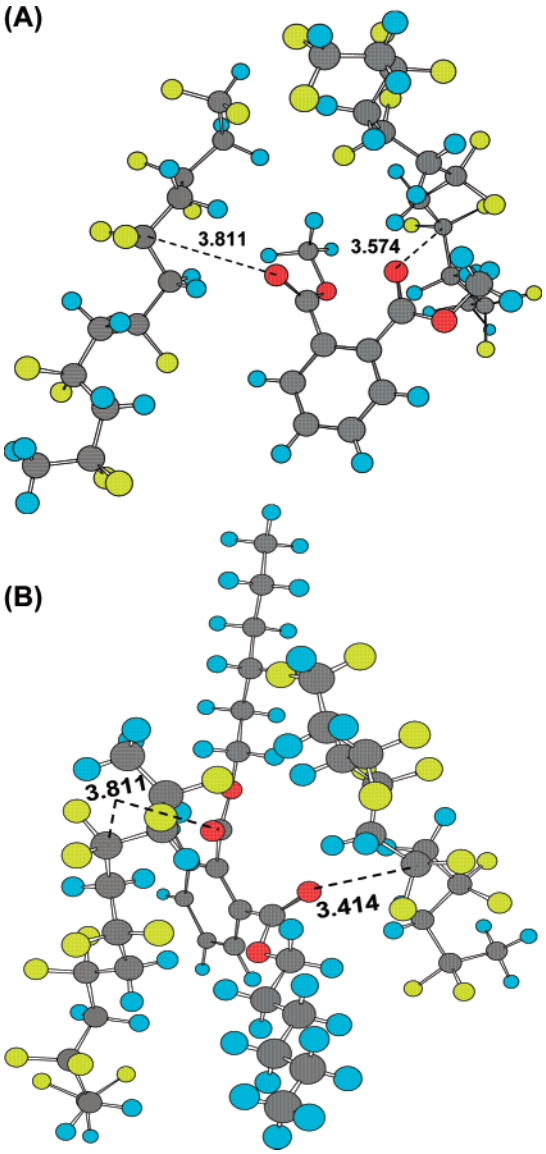

Figure 13. Molecular models of PVDF−phthalate complexes obtained from energy minimized electronic structure calculation (A) in DMP and (B) in DHP solvent showing the distance between nearest dipole in both side of the solvent.

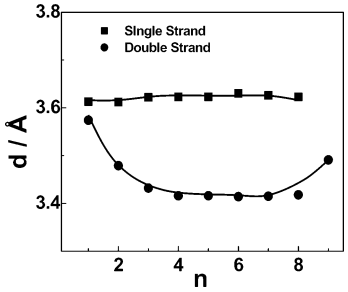

Figure 14. The shorter distance between two interactive dipoles in PVDF−phthalate complexes, shown above as a function of aliphatic chain length (*n*) considering single and double stranded models. The solid lines are arbitrarily drawn to show the nature of changes.

the experimental observation that the gelation rate increases up to $n = 6$. As the distance between the $>CF_2$ of PVDF and $>C=O$ of ester decreases, stronger complexation may occur up to $n = 6$ because the interaction between PVDF and phthalate is dipolar in nature. Obviously, the gelation rate will be enhanced gradually for stronger complexes. On the contrary, the dipole distance increases after $n = 6$; as a result, the formation of physical junction points may hampered causing no formation of gel from sol state. In summary, the modeling suggests that the interaction of PVDF with cis- form of phthalates remains same through out the series considered here and cannot account for the variation of gelation rate observed experimentally. On the other hand, in case of trans- form minimum distance of approach of phthalates toward PVDF chain initially decreases with chain length of the ester group of phthalate and then increases for $n > 6$, passing through a minimum for C_6 carbon chain length that strongly supports the experimental observations.

Hence, the structure, morphology, thermal behavior, scattering experiment, and modeling convoluted the gelation behavior, kinetics, and mechanism of PVDF gels in various phthalates, and this concept can be extended to other polymer−solvent pairs of similar interacting nature.

Conclusion

We have reported thermoreversible gelation of PVDF in various phthalates with wide range of aliphatic chain length ($n = 1-8$). Gelation kinetics as a function of PVDF concentrations as well as solution temperature was measured by using both TT and DLS methods. Both the techniques showed that the gelation rate increases with increasing aliphatic chain length of diesters. The differences in the gelation rates in phthalates have been explained in terms of further reorganization of 3D network structure even after physical gels formed. PVDF produces fibrillar morphology and the dimensions become thinner (lateral and width) with increasing aliphatic chain length. The crystallites are acting as a cross linking point during gelation of PVDF in phthalates and the crystallinity increases with higher homologue of phthalates causing the enhanced rate of gelation with increasing *n*. The scattering intensity decreases following Debye−Bueche model. Both the correlation length and characteristic wavelength (interlamellar distance) also increases with aliphatic chain length of diester. A model has been proposed how the lamella and crystallites are oriented inside the fibrils. The electronic structure calculation quantitatively predicts the rate of gelation observed experimentally, also accounts for no formation of gels beyond dihexyl phthalate.

Acknowledgment. The authors acknowledge the receipt of research funding from UGC-DAE CSR, Mumbai Centre (Project No. CSR/CD/MUM/CRS-M-116). The authors also acknowledge the kind support of Dr. D. K. Avasthi and Mr. Pawan K. Kulriya of IUAC, New Delhi during XRD measurements and Ausimont, Italy for supplying PVDF samples.

References and Notes

(1) Domszy, R. C.; Alamo, R.; Edwards, C. O; Mandelkern, L. *Macromolecules* **1986**, *19*, 310.
(2) Berghmans, H. In *Integration of Fundamental Polymer Science and Technology*; Lemstra, P. J., Kleintjens, L. A., Eds.; Elsevier Applied Science: London, 1988; Vol. 2, p 296.
(3) Guenet, J. M. In *Thermoreversible Gelation of Polymers and Biopolymers*; Academic Press: London, 1997.
(4) Paul, D. R. *J. Appl. Polym. Sci.* **1967**, *11*, 439.
(5) Kawanishi, K.; Komatsu M.; Inoue, T. *Polymer* **1987**, *28*, 980.
(6) Komatsu, M.; Inoue, T.; Miyasaka, K. *Polym. Sci. Polym. Phys. Ed.* **1986**, *24*, 303.
(7) Tazaki, M.; Wada, R.; Okabe, M.; Homma, T. *J. Appl. Polym. Sci.* **1997**, *65*, 1517.
(8) Hasegawa, R.; Kobayashi, M.; Tadokoro, H. *Polym. J.* **1972**, *3*, 593.
(9) Hasegawa, R.; Takahashi, Y.; Chatani, Y.; Tadokoro, H. *Polym. J.* **1972**, *3*, 600.
(10) Lando, J. B.; Olf, H. G.; Peterlin, A. *J. Polym. Sci., Part A-1* **1969**, *4*, 941.

(11) Kobayashi, M.; Tashiro, K.; Tadokoro, H. *Macromolecules* **1975**, *8*, 158.
(12) Basset, D. C. In *Development in Crystalline Polymers*; Basset, D. C., Ed.; Applied Science Publishers: London, 1982.
(13) Cho, J. W.; Song, H. Y.; Kim, S. Y. *Polymer* **1993**, *34*, 1024.
(14) Kim, B. S.; Baek, S. T.; Song, K. W.; Park, I. H.; Lee, J. O.; Nemoto, N. *J. Macromol. Sci. Part B* **2004**, *B43*, 741.
(15) Mal, S.; Maiti, P.; Nandi, A. K. *Macromolecules* **1995**, *28*, 2371.
(16) Mal, S.; Nandi, A. K. *Polymer* **1998**, *30*, 6301.
(17) Dikshit, A. K.; Nandi, A. K. *Macromolecules* **2000**, *33*, 2616.
(18) Dasgupta, D.; Nandi, A. K. *Macromolecules* **2005**, *38*, 6504.
(19) Dasgupta, D.; Manna, S.; Malik, S.; Rochas, C.; Guenet, J. M.; Nandi, A. K. *Macromolecules* **2005**, *38*, 5602.
(20) Dikshit, A. K.; Nandi, A. K. *Langmuir* **2001**, *17*, 3607.
(21) (a) Tanaka, T.; Hocker, L. O.; Benedek, G. B. *J. Chem. Phys.* **1973**, *59*, 5151. (b) Tanaka, T. *Phys. Rev. A* **1978**, *17*, 763.
(22) Munch, J. P.; Candau, S.; Hild, G. J. *Polym. Sci. Polym. Phys. Ed.* **1977**, *15*, 11.
(23) Munch, J. P.; Lemarechal, P.; Candau, S. *J. Phys.* **1977**, *38*, 1499.
(24) (a) Uhlenbeck, G. E.; Ornstein, L. S. *Phys. Rev.* **1930**, *36*, 823; McAdam, J. D. G.; King, T. A.; Knox, A. *Chem. Phys. Lett.* **1974**, *26*, 6. (b) Wun, K. L.; Carison, F. D. *Macromolecules* **1975**, *8*, 190.
(25) Adam M.; Delsanti, M. *Macromolecules* **1977**, *10*, 1229.
(26) Amis E. J.; Han, C. C. *Polymer* **1981**, *23*, 1403.
(27) Brown, W.; Nicolai, T. *Colloid Polym. Sci.* **1990**, *267*, 977.
(28) de Gennes P. G. *Scaling Concepts in Polymer Physics*; Cornell University Press: Ithaca, NY, 1979.
(29) Martin, J. E.; Wilcoxon, J.; Odinek, J. *Phys. Rev. A* **1991**, *43*, 858.
(30) Wu, C.; Ngai, T. *Polymer* **2004**, *45*, 1739.
(31) Narayanan, J.; Deotare, V. W.; Bandyapadhyay, R.; Sood, A. K. *J. Colloid Interf. Sci.* **2002**, *245*, 267.
(32) Pusey, P. N.; van Megen, W. *Physica A* **1989**, *157*, 705.
(33) Joosten, J. G. H.; Gelade, E. T. F.; Pusey, P. N. *Phys. Rev. A* **1990**, *42*, 2161.
(34) Xue, J. Z.; Pine, D. J.; Milner, S. T.; Wu, X. I.; Chaikin, P. M. *Phys. Rev. A* **1992**, *46*, 6550.
(35) (a) Mata, J.; Varade, D.; Ghosh, G.; Bahadur, P. *Colloids Surf. A* **2004**, *245*, 69. (b) Takata, S.; Norisuye, T.; Tanaka, N.; Shibayama, M. *Macromolecules* **2000**, *33*, 5470.
(36) Kanaya, T.; Ohkura, M.; Kaji, K.; Furusaka, M.; Misawa, M. *Macromolecules* **1994**, *27*, 5609.
(37) Takcshita. H.; Kanaya, T.; Nishida, K.; Kaji, K.; Takahashi, T.; Hashimoto, M. *Phys. Rev. E* **2000**, *61*, 2125.
(38) Pecora, R. *Dynamic Light Scattering: Applications of Photon Correlation Spectroscopy*; Plenum Press: NY, 1985.
(39) Bohidar, H. B. *Curr. Sci.* **2001**, *80*, 1008.
(40) Aswal, V. K.; Goyal, P. S. *Curr. Sci.* **2000**, *79*, 947.
(41) Martin, J. E.; Wilcoxon, J. P. *Phys. Rev. Lett.* **1988**, *61*, 373.
(42) Takeshita, H.; Kanaya, T, Nishida, K.; Kaji, K. *Macromolecules* **1999**, *32*, 7815.
(43) Miyazaki, S.; Endo, H.; Karino, T.; Haraguchi, K.; Shibayama, M. *Macromolecules* **2007**.
(44) Eldridge, J. E.; Ferry, J. D. *J. Phys. Chem.* **1964**, *58*, 992.
(45) (a) Stauffer, D.; Coniglio, A.; Adam, M. *Advances in Polymer Science*; Dusek, K., Ed.; Springer-Verlag: Berlin, 1982; Vol. 44, p 103.
(46) Welch, G. J.; Miller, R. L. *J. Polym. Sci.* **1976**, *B14*, 1683.
(47) Hasegawa, R.; Takahashi, Y.; Chatani, Y. *Polym. J.* **1972**, *3*, 600.
(48) Kobayashi, M.; Tashiro, K.; Tadokoro, H. *Macromolecules* **1975**, *8*, 158.
(49) Belke, R. E.; Cabasso, I. *Polymer* **1988**, *29*, 1831.
(50) Enomoto, S.; Kawai, Y.; Sugita, M. *J. Polym Sci.* **1968**, *A26*, 861.